Theoretical investigation of phenomena in the closed Raman-driven four-level symmetrical model

Hong Yuan Ling
Department of Chemistry and Physics, Rowan College of New Jersey, Glassboro, New Jersey 08028
(Received 17 September 1993)

We construct a solution to the linear complex absorption coefficient for the closed Raman-driven four-level symmetrical model. We derive, from this solution, asymptotic expressions for the spectra around and away from the two-photon resonance in the absence as well as in the presence of the Doppler broadening. They are used for the derivations of analytical conditions and the discussion of the physical origins of various phenomena that do not appear in the traditional two-level system.

PACS number(s): 42.50.Gy, 42.50.Hz, 42.65.An

I. INTRODUCTION

Recent study in the area of quantum optics indicates that the population inversion is not a necessary condition for producing laser light [1–8]. Lasing without population inversion has been proven to be possible if one of two lasing transition levels (either high or lower) is a doublet with a sufficient coherence. The coherence between the doublet can be established by different schemes: their relaxation to the same continuum [3]; coherent excitation or microwave interaction [4]; their interaction with an auxiliary level via Raman field [5,6] or double Raman fields [7,8]. The phenomenon of lasing without population inversion is governed by the imaginary part of the complex polarization. Study of both the imaginary and the real parts of the complex polarization in the same medium reveals unusual dispersion-absorption relationships in the sense that they can depart from the Kramers-Kronig rule. Harris and co-workers [9,10] have pointed out that in a three-level model the index of refraction can be zero but have a large slope where absorption vanishes via a strong electromagnetic field. Fleischhauer *et al.* [11] have proven theoretically that the largest index of refraction without absorption is possible in virtually every lasing without a population-inversion model.

In this paper, we focus our study on the closed Raman-driven four-level model, which was originally proposed by Narducci *et al.* [5] for the purpose of demonstrating lasing without inversion. Figure 1 is its schematics. The ground state consists of two closely spaced levels labeled 1 and 2. The frequency ω of the weak probe is set to be close to the atomic transition frequencies between the ground levels and the upper level 3. The auxiliary level 4 is coupled to the ground levels through dipole transitions 4-2 and 4-1 by a strong Raman field of frequency ω_r. Several papers [5,6,12] have attempted to explore its physical origin of lasing without inversion. Shu *et al.* [13] and Scully *et al.* [14] have developed a laser theory for this model. Fleischhauer *et al.* [11] have proven that it is possible to have the largest index of refraction without absorption, and has implied, in the same paper, the possibility of electromagnetically induced transparency. Doppler effects have also been briefly discussed in Refs. [11] and [15].

This paper, compared with other work, has several important features. First, we have organized the solution to the linear complex absorption coefficient of the symmetrical model in such a way that the conditions for various phenomena can be derived analytically. Second, besides the role of the lower-level coherence, we identify the role that the upper-level coherence plays in leading to efficient lasing without inversion, that is, by very small pumping rate, and other phenomena. To illustrate this point, we indicate that a ground doublet creates various indistinguishabilities among different pathways. Specifically, when a photon of frequency ω is emitted or absorbed, one cannot tell whether it is caused by 3-1 or 3-2 single-photon transitions, or whether it is caused by 3-1-4 or 3-2-4 two-photon transitions. The former type of indistinguishability is due to the lower-level coherence, while the latter is mainly due to the upper-level coherence. Under suitable conditions, these pathways will interfere, resulting in an efficient lasing without inversion and other phenomena. Third, we point out that the population difference that is present in the complex linear-absorption coefficient in the traditional two-level system is now replaced by a complex number that contains not only the diagonal but also off-diagonal density matrix elements. The real part of this complex number produces the traditional Lorentzian type of absorption-dispersion relation, while the imaginary part of this complex number produces the absorptionlike dispersion and dispersionlike absorption. For convenience, in this paper we call the latter absorption-dispersion relation Rayleigh wing type. We

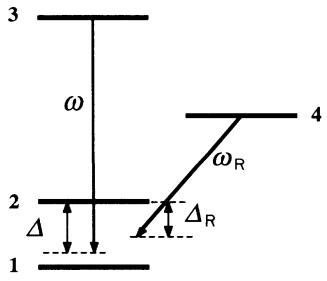

FIG. 1. Schematics of the Raman-driven four-level model.

attribute the absorption-dispersion relations such as the largest index refraction without absorption to the interplay between the Lorentzian-type and Rayleigh-wing-type spectra.

The paper is organized as follows. In Sec. II, we construct a simple analytical solution to the linear complex absorption coefficient for the symmetrical Raman-driven four-level model. We generate, from this solution, asymptotic expressions for the spectra with and without Doppler broadening. In Sec. III, we apply the theories developed in Sec. II to derive analytical criteria that lead to different phenomena, and provide physical interpretations to their origins as well. Section IV summaries the major results.

II. THEORY

A. Homogeneously broadened medium

We take the usual approach to find the polarization of the Raman-driven model subject to the two plane waves

$$F(z,t)=\tfrac{1}{2}Fe^{-i\omega t+ikz}+\text{c.c.} ,$$

$$F_R(z,t)=\tfrac{1}{2}F_R e^{-i\omega_R t+ik_R z}+\text{c.c.} ,$$

where F and F_R are the slowly varying functions of time t and distance z, k and k_R are the wave vectors, and subscript R stands for the Raman field. In the rotational-wave approximation, we can express the nonzero Hamiltonian elements H'_{ij} in the interaction picture as

$$\begin{aligned} &H'_{32}=\hbar E e^{-i\Delta t}e^{+ikz},\quad H'_{31}=\hbar E e^{i(\Omega_{21}-\Delta)t}e^{+ikz} ,\\ &H'_{43}=\hbar E_R e^{-i\Delta_R t}e^{+ik_R z} ,\\ &H'_{41}=\hbar E_R e^{i(\Omega_{21}-\Delta_R)t}e^{+ik_R z} , \end{aligned} \tag{2.1}$$

where Ω_{ij} stands for the atomic transition frequency from level i to j, Δ (equal to $\omega-\Omega_{32}$) and Δ_R (equal to $\omega_R-\Omega_{42}$) represents the detunings of the probe and the Raman field with respect to level 2, respectively, and $\hbar$ is the Planck constant. In reaching Eq. (2.1), we have introduced the Rabi equivalent field amplitudes

$$E=\frac{\mu F}{2\hbar},\quad E_R=\frac{\mu_R F_R}{2\hbar} ,$$

where we have already assumed that 3↔2 and 3↔1 transitions have the same dipole moment of μ, and 4↔2 and 4↔1 transitions have the same dipole moment of μ_R. This interaction induces a polarization oscillating at the frequency of the weak probe of the similar form

$$P(z,t)=\tfrac{1}{2}Pe^{-i\omega+ikz}+\text{c.c.} ,$$

where P is a slowly varying function. The connection between the field and the polarization is closed through the Maxwell's wave equations. For the slowly varying amplitudes and in the steady state, the Maxwell's wave equations are reduced to the coupled wave equations. In particular, the equation for the amplitude of the weak signal becomes

$$\frac{dE}{dz}=-i\frac{k\mu}{4\varepsilon\hbar}P\equiv\bar{\alpha}E ,$$

where ε is the permittivity of the host medium, and the complex absorption (gain) coefficient is defined as

$$\bar{\alpha}=i\frac{k\mu}{4\varepsilon\hbar}\frac{P}{E} . \tag{2.2}$$

The evolution of the atomic variables is governed by the density-matrix equation. This equation, in the interaction picture, takes the form

$$\frac{\partial\rho'}{\partial t}=-\frac{i}{\hbar}[H',\rho']+\Lambda\rho' , \tag{2.3}$$

where ρ' stands for the density-matrix operator in the interaction picture, and $\Lambda\rho'$ describes the irreversible contributions due to spontaneous decays, other possible line-broadening mechanisms, and the incoherent pump to level 3. By expanding Eq. (2.3) in terms of newly defined matrix density elements

$$\begin{aligned} &\rho_{32}=\rho'_{32}e^{+i\Delta t}e^{-ikz},\quad \rho_{31}=\rho'_{31}e^{-i(\Omega_{21}-\Delta)t}e^{-ikz} ,\\ &\rho_{42}=\rho'_{42}e^{+i\Delta_R t}e^{-ik_R z} ,\\ &\rho_{41}=\rho'_{41}e^{-i(\Omega_{21}-\Delta_R)t}e^{-ik_R z},\quad \rho_{21}=\rho'_{21}e^{-i\Omega_{21}t} ,\\ &\rho_{34}=\rho'_{34}e^{i(\Delta-\Delta_R)t},\quad \rho_{ii}=\rho'_{ii} , \end{aligned}$$

we can easily write the component equations of motion as

$$\begin{aligned} \frac{d\rho_{33}}{dt}&=-(W_{32}+W_{31}+W_{34})\rho_{33}+\Gamma_{23}\rho_{22}\\ &\quad+\Gamma_{13}\rho_{11}+i(E^*\rho_{32}+E^*\rho_{31}-\text{c.c.}) ,\\ \frac{d\rho_{44}}{dt}&=-(W_{42}+W_{41})\rho_{44}+W_{34}\rho_{33}\\ &\quad+i(E_R^*\rho_{42}+E_R^*\rho_{41}-\text{c.c.}) ,\\ \frac{d\rho_{22}}{dt}&=-(W_{21}+\Gamma_{23})\rho_{22}+W_{12}\rho_{11}+W_{32}\rho_{33}\\ &\quad+W_{42}\rho_{44}+i(E\rho_{23}+E_R\rho_{24}-\text{c.c.}) ,\\ \frac{d\rho_{11}}{dt}&=-(W_{12}+\Gamma_{13})\rho_{11}+W_{21}\rho_{22}+W_{31}\rho_{33}\\ &\quad+W_{41}\rho_{44}+i(E\rho_{13}+E_R\rho_{14}-\text{c.c.}) ,\\ \frac{d\rho_{32}}{dt}&=-\gamma_{32}\rho_{32}+i\Delta\rho_{32}-iE(\rho_{22}-\rho_{33})\\ &\quad-iE\rho_{12}+iE_R\rho_{34} ,\\ \frac{d\rho_{31}}{dt}&=-\gamma_{31}\rho_{31}-i(\Omega_{21}-\Delta)\rho_{31}\\ &\quad-iE(\rho_{11}-\rho_{33})-iE\rho_{21}+iE_R\rho_{34} ,\\ \frac{d\rho_{42}}{dt}&=-\gamma_{42}\rho_{42}+i\Delta_R\rho_{42}-iE_R(\rho_{22}-\rho_{44})\\ &\quad-iE_R\rho_{12}+iE\rho_{43} ,\\ \frac{d\rho_{41}}{dt}&=-\gamma_{41}\rho_{41}-i(\Omega_{21}-\Delta_R)\rho_{41}\\ &\quad-iE_R(\rho_{11}-\rho_{44})-iE_R\rho_{21}+iE\rho_{43} ,\\ \frac{d\rho_{21}}{dt}&=-\gamma_{21}\rho_{21}-i\Omega_{21}\rho_{21}+iE\rho_{23}\\ &\quad-iE^*\rho_{31}+iE_R\rho_{24}-iE_R^*\rho_{41} ,\\ \frac{d\rho_{34}}{dt}&=-\gamma_{34}\rho_{34}+i(\Delta-\Delta_R)\rho_{34}-iE\rho_{24}\\ &\quad+iE_R^*\rho_{32}-iE\rho_{14}+iE_R^*\rho_{31} ,\\ \rho_{ij}&=\rho_{ji},\quad i\neq j , \end{aligned} \tag{2.4}$$

where W_{ij} stands for the population decay rate from level i to level j, Γ_{ij} the incoherent pumping rate from level i to j, and γ_{ij} the dephasing rate of the off-diagonal element between levels i and j. The slowly varying polarization is expressed by

$$P=N\mu(\rho_{32}+\rho_{31}) , \tag{2.5}$$

where N is the atomic density. By substituting P in Eq. (2.2) with Eq. (2.5), we find that

$$\alpha=-i\frac{(\rho_{32}+\rho_{31})}{E} , \tag{2.6}$$

where α is the complex absorption coefficient $\bar{\alpha}$ scaled to $4\varepsilon\hbar/(Nk\mu^2)$. The linear response of α to the weak probe can be derived by taking advantage of the intensity difference between the Raman field and weak probe. Here we follow the method in [16] to obtain a solution correct to all orders of Raman field, but linear order of weak probe. This solution under arbitrary parameters has a very complex form and, therefore, is not suitable for analytical study. For this reason, we leave it in Appendix A. For simplicity, here we restrict our study only to the symmetrical model based on the assumptions $\Gamma_{23}=\Gamma_{13}\equiv\Gamma$, $\gamma_{32}=\gamma_{31}\equiv\gamma$, $W_{32}=W_{31}\equiv W$, $W_{42}=W_{41}\equiv W_R$, $\gamma_{42}=\gamma_{41}\equiv\gamma_R$, $W_{21}=W_{12}$, $\Delta_R=\Omega_{21}/2$. By taking advantages of various symmetries implied in these assumptions, we are able to find a solution in the form of

$$\alpha=\frac{[-\gamma-i(\Omega_{21}-\Delta)]S_1+(-\gamma+i\Delta)S_2}{(-\gamma+i\Delta)[-\gamma-i(\Omega_{21}-\Delta)]-\dfrac{-2\gamma+i(2\Delta-\Omega_{21})}{\gamma_{34}-i(\Delta-\Delta_R)}I_R} , \tag{2.7}$$

where

$$S_1=(\rho_{gg}^{(0)}-\rho_{33}^{(0)})+\rho_{12}^{(0)}-\mathcal{R}_{34}^{(0)}/[\gamma_{34}-i(\Delta-\Delta_R)] , \tag{2.8a}$$

$$S_2=(\rho_{gg}^{(0)}-\rho_{33}^{(0)})+\rho_{21}^{(0)}-\mathcal{R}_{34}^{(0)}/[\gamma_{34}-i(\Delta-\Delta_R)] , \tag{2.8b}$$

and $I_R=E_R^*E_R$.

The zeroth-order solutions appearing in S_1 and S_2 are summarized as

$$\rho_{33}^{(0)}=n_3\frac{1+\dfrac{2I_R\lambda}{(\delta^2+\lambda^2)W_R}}{1+\dfrac{2I_R\lambda}{(\delta^2+\lambda^2)W_R}d} ,$$

$$\rho_{gg}^{(0)}=n_g\frac{1+\dfrac{2I_R\lambda}{(\delta^2+\lambda^2)W_R}}{1+\dfrac{2I_R\lambda}{(\delta^2+\lambda^2)W_R}d}(=\rho_{11}^{(0)}=\rho_{22}^{(0)}) ,$$

$$\rho_{44}^{(0)}=\frac{n_4+n_g\dfrac{2I_R\lambda}{(\delta^2+\lambda^2)W_R}}{1+\dfrac{2I_R\lambda}{(\delta^2+\lambda^2)W_R}d} , \tag{2.9}$$

$$\rho_{21}^{(0)}=-2I_R\frac{\rho_{gg}^{(0)}-\rho_{44}^{(0)}}{(\gamma_{21}+i\Omega_{21})(\lambda+i\delta)} ,$$

$$\mathcal{R}_{34}^{(0)}\equiv-iE_R(\rho_{24}^{(0)}+\rho_{14}^{(0)})$$

$$=I_R\frac{2\lambda}{\lambda^2+\delta^2}(\rho_{gg}^{(0)}-\rho_{44}^{(0)}),\quad \rho_{12}^{(0)}=\rho_{21}^{(0)*} ,$$

where

$$n_1=n_2\equiv n_g=\frac{W_R(2W+W_{34})}{\Gamma(W_{34}+2W_R)+2W_R(2W+W_{34})} ,$$

$$n_3=\frac{2\Gamma W_R}{\Gamma(W_{34}+2W_R)+2W_R(2W+W_{34})} , \tag{2.10}$$

$$n_4=\frac{\Gamma W_{34}}{\Gamma(W_{34}+2W_R)+2W_R(2W+W_{34})}$$

are the equilibrium populations of ground levels, level 3, and level 4 in the absence of any coherent perturbations;

$$d=\frac{W_R[2\Gamma+3(2W+W_{34})]}{\Gamma(W_{34}+2W_R)+2W_R(2W+W_{34})} \tag{2.11}$$

is a unitless number; and finally

$$\delta=\Delta_R-\frac{2I_R\Omega_{21}}{\gamma_{21}^2+\Omega_{21}^2},\quad \lambda=\gamma_R+\frac{2I_R\gamma_{21}}{\gamma_{21}^2+\Omega_{21}^2} . \tag{2.12}$$

Equation (2.7) indicates that α is a coherent superposition of 3-1-4 and 3-2-4 pathways, which are represented by S_1 and S_2, respectively. The polarization of each pathway is made up of three source terms: single photon, lower-level coherence, and upper-level coherence. To understand the contribution from the upper-level coherence, let us express $\rho_{34}^{(1)}$, in terms of zeroth-order solutions, as

$$\rho_{34}^{(1)}=-iE\frac{\rho_{24}^{(0)}+\rho_{14}^{(0)}}{\gamma_{34}-i(\Delta-\Delta_R)}+iE_R^*\frac{\rho_{32}^{(1)}}{\gamma_{34}-i(\Delta-\Delta_R)}$$

$$+iE_R^*\frac{\rho_{31}^{(1)}}{\gamma_{34}-i(\Delta-\Delta_R)} . \tag{2.13}$$

Each term in Eq. (2.13) makes a very different contribution to the linear polarization. The first term becomes one of the source terms defined as $\mathcal{R}_{34}^{(0)}$, signifying that it originates from upper-level coherence, the second and third terms cause an ac-Stark shift [the denominator of Eq. (2.7)] and a coupling between $\rho_{31}^{(1)}$ and $\rho_{32}^{(1)}$. One of the

nice features of Eq. (2.9) is that the effect of the Raman field has been effectively dressed into the two variables λ and δ [Eq. (2.12)]. Such an organization enables us to easily identify the high-intensity limit

$$I_R \gg \frac{\gamma_R}{2\gamma_{21}}(\gamma_{21}^2+\Omega_{21}^2) , \tag{2.14}$$

as well as to obtain the solutions under this limit,

$$\begin{aligned}
&\rho_{33}^{(0)}(\infty)=n_3\frac{1+\gamma_{21}/W_R}{1+\gamma_{21}d/W_R},\quad \rho_{gg}^{(0)}(\infty)=n_g\frac{1+\gamma_{21}/W_R}{1+\gamma_{21}d/W_R} ,\\
&\rho_{44}^{(0)}(\infty)=\frac{n_4+n_g\gamma_{21}/W_R}{1+\gamma_{21}d/W_R} ,\\
&\rho_{21}^{(0)}(\infty)=-[\rho_{gg}^{(0)}(\infty)-\rho_{44}^{(0)}(\infty)] ,\\
&\mathcal{R}_{34}^{(0)}(\infty)=\gamma_{21}[\rho_{gg}^{(0)}(\infty)-\rho_{44}^{(0)}(\infty)] ,
\end{aligned} \tag{2.15}$$

where ∞ stands for high Raman intensity limit.

We now derive from Eq. (2.7) two special forms of complex absorption coefficients. One is derived under the condition that the probe frequency is tuned in the neighborhood of two-photon resonance, that is, $\Delta\approx\Delta_R$. The other is complementary to the first one in the sense that the probe frequency is away from the two-photon resonance, that is, $\Delta\gg\Delta_R$. We find the first one by replacing Δ in Eq. (2.7) with Δ_R, as

$$\alpha=2\frac{A_1\gamma+\Delta_R\,\mathrm{Im}(\rho_{12}^{(0)})}{\Delta_R^2+\gamma^2[1+2I_R/(\gamma\gamma_{34})]} , \tag{2.16}$$

where

$$A_1=A_2+\mathcal{R}_{34}^{(0)}/\gamma_{34} , \tag{2.17a}$$

$$A_2=-[(\rho_{gg}^{(0)}-\rho_{33}^{(0)})+\mathrm{Re}(\rho_{12}^{(0)})] , \tag{2.17b}$$

and the second one by ignoring Δ_R and Ω_{21} in Eq. (2.7), as

$$\alpha=\frac{-g_R+ig_L}{\Delta-d_0+iR}+\frac{g_R+ig_L}{\Delta+d_0+iR} , \tag{2.18}$$

where

$$\begin{aligned}
&g_R=\frac{\gamma_{34}A_1-A_2R}{d},\quad g_L=A_2 ,\\
&d_0=\sqrt{2I_R-[(\gamma_{34}-\gamma)/2]^2},\quad R=\frac{\gamma_{34}+\gamma}{2} ,
\end{aligned} \tag{2.19}$$

of course, under the condition that $I_R>0.125(\gamma_{34}-\gamma)^2$. Equation (2.18) can be further separated into absorption and dispersion spectra as

$$\mathrm{Re}(\alpha)=\frac{-g_R(\Delta-d_0)+g_LR}{(\Delta-d_0)^2+R^2}+\frac{g_R(\Delta+d_0)+g_LR}{(\Delta+d_0)^2+R^2} , \tag{2.20}$$

$$\mathrm{Im}(\alpha)=\frac{g_RR+g_L(\Delta-d_0)}{(\Delta-d_0)^2+R^2}+\frac{-g_RR+g_L(\Delta+d_0)}{(\Delta+d_0)^2+R^2} . \tag{2.21}$$

Note that although Eqs. (2.18), (2.20), and (2.21) are derived under the condition that $\Delta\gg\Delta_R$, they apply to any probe frequency if the two lower levels are degenerate.

B. Doppler-broadened medium

When an atom moving with velocity v interacts with the fields, both the field frequency ω_0 and the Raman frequency ω_{R0}, in the perspective of the atoms, are Doppler shifted to new values ω and ω_R given by

$$\omega=\omega_0+\frac{\omega_0 v}{c},\omega_R=\omega_{R0}+\frac{\omega_{R0}v}{c} , \tag{2.22}$$

where c is the speed of light in vacuums. The distribution of atoms over velocity is a well known Gaussian function. By expressing the velocity in terms of probe frequency, we can transform the distribution over velocity into the distribution over frequency as

$$P(\Delta)=\frac{1}{\sqrt{\pi\,\delta\omega^2}}\exp\left[-\frac{(\Delta-\Delta_0)^2}{\delta\omega^2}\right] , \tag{2.23}$$

where $\Delta_0=\omega_0-\omega_{32}$ and $\delta\omega$, proportional to the Doppler width, measures the degree of Doppler broadening. We note because the frequency of the Raman field seen by the atoms varies, we cannot discuss this problem from the symmetrical model, where Δ_R is fixed at $\Omega_{21}/2$. Therefore, without special assumptions, the complex absorption coefficient in the presence of Doppler broadening, $\alpha(\Delta_0,\Delta_{R0},\delta\omega)$, has to be calculated numerically by the integral

$$\alpha(\Delta_0,\Delta_{R0},\delta\omega)=\frac{1}{\sqrt{\pi\,\delta\omega^2}}\times\int_{-\infty}^{+\infty}\alpha(\Delta,\Delta_R)\exp\left[-\frac{(\Delta-\Delta_0)^2}{\delta\omega^2}\right]d\Delta , \tag{2.24}$$

where $\Delta_{R0}=\omega_{R0}-\omega_{42}$ and $\alpha(\Delta,\Delta_R)$ is obtained numerically from Eq. (A1). We note that Δ_R is not an independent variable. It should be replaced by

$$\Delta_R=\Delta_{R0}+\frac{\omega_{R0}}{\omega_0}(\Delta-\Delta_0) ,$$

which is obtained via the two relations in Eq. (2.22).

In the following, we derive two analytical solutions under special conditions. Before defining the assumptions unique to each solution, we present two assumptions that are common to both solutions. First, we require that the Gaussian distribution function in Eq. (2.24) be replaced with the Lorentzian function

$$\frac{1}{\pi}\frac{\delta\omega}{(\Delta-\Delta_0)^2+\delta\omega^2} . \tag{2.25}$$

The solutions obtained with the Gaussian function have to be expressed in terms of complex error functions and, thus, are not useful for analytical discussions. Second, as usual, we assume that $\Delta_{R0}(=\Omega_{21}/2)$ is small. The special

conditions to the first solution are that first, the probe frequency is tuned to the frequency regime of two-photon resonance, and second, the Doppler broadening of the Raman field in the zeroth-order solution is ignored. Our argument regarding the second assumption is that the two-photon process, that is, 1-4-2, should dominate the single-photon process when a strong Raman field interacts with both 1-4 and 2-4 atomic transitions. Because the transition frequencies of 1-4 and 2-4 are very close to each other, the two-photon resonance condition, determined by the difference between the two transition frequencies, is insensitive to the Doppler broadening of the Raman field. We now apply these assumptions to Eq. (2.7), and transform it into

$$\alpha(\Delta,\Delta_R)=2\frac{-A_1\gamma_{34}+i\,\delta\omega f A_2}{-(\gamma\gamma_{34}+2I_R)+f(\Delta-\Delta_0)^2+i(\gamma_{34}+\gamma f)(\Delta-\Delta_0)}\ , \tag{2.26}$$

where $f=(1-\omega_{R0}/\omega_0)$. We next replace $\alpha(\Delta,\Delta_R)$ and the Gaussian distribution in Eq. (2.24) with Eqs. (2.26) and (2.25), respectively, and solve it by the method of contour integration. We finally obtain the first solution in the form of

$$\alpha(\Delta_0,\Delta_{R0},\delta\omega)=2\frac{A_1\gamma_{34}+f\,\delta\omega A_2}{\gamma\gamma_{34}+2I_R+(\gamma_{34}+f\gamma)\delta\omega+f\,\delta\omega^2}\ . \tag{2.27}$$

The unique conditions for the second solution are that first, the probe frequency is far from that of the two-photon resonance regime, and second, the Raman frequency is much smaller than the probe frequency, but still much larger than Ω_{21}. Under these assumptions, the Doppler broadening of the Raman field can be ignored both in the zeroth-order and in the first-order solutions. Thus, we replace $\alpha(\Delta,\Delta_R)$ and the Gaussian distribution with Eq. (2.18) and Eq. (2.25), and solve it again by the contour integration method. We are able to obtain three equations identical to Eqs. (2.18), (2.20), and (2.21) except that R now is replaced with $R+\delta\omega$.

III. DISCUSSION

Sections III A–III C deal with the homogeneously broadened medium, while Sec. III D is devoted to the Doppler-broadened medium.

A. Conditions for efficient lasing without inversion

It is not difficult to see that the absorption curve is an even function of $\Delta-\Delta_R$, and therefore reaches an extreme when $\Delta=\Delta_R$. Furthermore, computer simulation indicates that the medium exhibits gain only when this extreme becomes positive. For this reason, we derive the lasing condition by setting Eq. (2.16) to be positive, that is,

$$A_1\gamma+\Delta_R\,\mathrm{Im}(\rho_{12}^{(0)})>0\ , \tag{3.1}$$

which, after first, A_1 is replaced with Eqs. (2.17) and (2.18) and second, the off-diagonal density elements are replaced with relations in Eq. (2.9), is transformed into

$$-\gamma(\rho_{gg}^{(0)}-\rho_{33}^{(0)})-2I_R\frac{\gamma(2\Delta_R\delta-\gamma_{21}\lambda)+\Delta_R(\gamma_{21}\delta+2\Delta_R\lambda)}{(\gamma_{21}^2+\Omega_{21}^2)(\lambda^2+\delta^2)}(\rho_{gg}^{(0)}-\rho_{44}^{(0)})+2I_R\frac{\lambda\gamma}{\gamma_{34}(\lambda^2+\delta^2)}(\rho_{gg}^{(0)}-\rho_{44}^{(0)})>0\ . \tag{3.2}$$

By replacing the diagonal elements in Eq. (3.2) with relations in Eq. (2.9), we can express Eq. (3.2) in terms of Raman intensity as a quadratic inequality

$$a_L I_R^2+b_L I_R+c>0\ , \tag{3.3}$$

where

$$\begin{aligned}
a_L&=-4\gamma(1+\gamma_{21}/W_R)(n_g-n_3)\\
&\quad+4\gamma(1+\gamma_{21}/\gamma_{34})(n_g-n_4)\ ,\\
b_L&=-2\gamma[2\gamma_R\gamma_{21}-\Omega_{21}\Delta_R)\\
&\quad+\gamma_R(\gamma_{21}^2+\Omega_{21}^2)/W_R](n_g-n_3)\\
&\quad-2[\gamma(2\Delta_R^2-\gamma_{21}\gamma_R)+\Delta_R^2(\gamma_{21}+2\gamma_R)\\
&\quad-\gamma_R\gamma(\gamma_{21}^2+\Omega_{21}^2)/\gamma_{34}](n_g-n_4)\ ,\\
c_L&=-\gamma(\Delta_R^2+\gamma_R^2)(\gamma_{21}^2+\Omega_{21}^2)(n_g-n_3)\ .
\end{aligned}$$

Because $c_L<0$, inequality (3.3) can be further decomposed into two simultaneous inequalities,

$$\begin{aligned}
a_L&=-4\gamma(1+\gamma_{21}/W_R)(n_g-n_3)\\
&\quad+4\gamma(1+\gamma_{21}/\gamma_{34})(n_g-n_4)>0
\end{aligned} \tag{3.4}$$

and

$$I_R>I_{R\mathrm{th}}^{(1)}=(-b_L+\sqrt{b_L^2-4a_Lc_L})/(2a_L)\ . \tag{3.5}$$

The physical origin of the gain can be traced back to the lower-level coherence represented by the second term in Eq. (3.2), and the upper-level coherence represented by the third term in Eq. (3.2). The former becomes a gain only if the Raman field is sufficiently high. By comparison, the latter is always a gain no matter how weak the Raman field. Note that the contribution due to the upper-level coherence in the traditional upside-down

anti-Stokes model (the same as in Fig. 1 except that the ground doublet is replaced with a singlet) consists of terms associated with not only $(\rho_{gg}^{(0)}-\rho_{44}^{(0)})$ but also $(\rho_{33}^{(0)}-\rho_{gg}^{(0)})$ and, therefore, becomes positive only under certain conditions. In the current model, as a result of the coherent superposition of 3-1-4 and 3-2-4 symmetrical two-photon pathways, the terms attached to $(\rho_{33}^{(0)}-\rho_{gg}^{(0)})$ are canceled out, leaving the upper-level coherence contribution an unconditional gain proportional to $(\rho_{gg}^{(0)}-\rho_{44}^{(0)})$. One can easily verify that Eq. (3.2), in the high-intensity limit, becomes

$$-\gamma[\rho_{gg}^{(0)}(\infty)-\rho_{33}^{(0)}(\infty)]+\gamma[\rho_{gg}^{(0)}(\infty)-\rho_{44}^{(0)}(\infty)] +\gamma\gamma_{21}/\gamma_{34}[\rho_{gg}^{(0)}(\infty)-\rho_{44}^{(0)}(\infty)]>0 , \tag{3.6}$$

which, after the zeroth-order populations are replaced with Eq. (2.15), turns out to be the same as Eq. (3.4).

The threshold pumping rate can be derived from Eq. (3.4) by replacing n_g, n_3, and n_4 with Eq. (2.10), and the off-diagonal decay rates with

$$\gamma_{21}=\tfrac{1}{2}(2\Gamma+2W_{12}),\quad \gamma_{34}=\tfrac{1}{2}(2W+2W_R+W_{34}) ,$$
$$\gamma=\tfrac{1}{2}(2W+\Gamma+W_{12}),\quad \gamma_R=\tfrac{1}{2}(2W_R+\Gamma+W_{12}) , \tag{3.7}$$

assuming the decays are purely radiative. These substitutions turn Eq. (3.4) into

$$a_\Gamma\Gamma^2+b_\Gamma\Gamma+c_\Gamma>0 , \tag{3.8}$$

where

$$a_\Gamma=2(W+W_R),\quad c_\Gamma=-(2W+W_{34})(W+0.5W_{34})W_{21} ,$$
$$b_\Gamma=2W_R^2+2W_R(W+W_{21})-2W^2 +W(2W_{21}-3W_{34})-W_{34}^2 .$$

From Eq. (3.8) we obtain a threshold pumping rate of

$$\Gamma_{\rm th}^{(1)}=\frac{-b_\Gamma+\sqrt{b_\Gamma^2-4a_\Gamma c_\Gamma}}{2a_\Gamma} . \tag{3.9}$$

Figure 2 shows $\Gamma_{\rm th}^{(1)}$ as a function of W_R for different

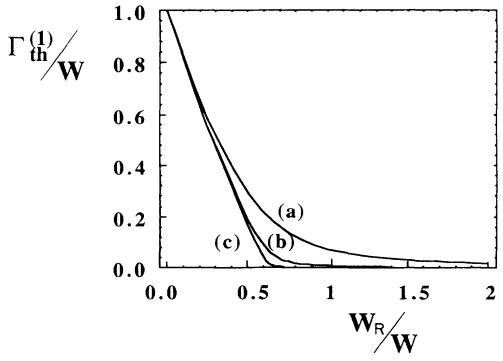

FIG. 2. Threshold pumping rate for amplification, $\Gamma_{\rm th}^{(1)}$, as a function of W_R with different W_{21}. The parameters are $W=1$, $W_{34}=0.0001$, and (a) $W_{21}=0.1$; (b) $W_{21}=0.01$; (c) $W_{21}=0.001$.

W_{21}. We note that although a lower pumping rate is required to produce a lasing effect as W_R increases and W_{21} decreases (more coherent), only if W_R exceeds a certain threshold can $\Gamma_{\rm th}^{(1)}$ be dramatically reduced by employing atomic systems of small W_{21}, which is usually true because the $2\leftrightarrow1$ transition is dipole forbidden. We now derive this threshold value for W_R from Eq. (3.8). It is not difficult to see that $\Gamma_{\rm th}^{(1)}$ can be approximated as

$$\Gamma_{\rm th}^{(1)}\approx\frac{-b_\Gamma+|b_\Gamma|-2a_\Gamma c_\Gamma/|b_\Gamma|}{2a_\Gamma} ,$$

because c_L, proportional to W_{21}, is much smaller than b_L. Thus, $\Gamma_{\rm th}^{(1)}$, depending on whether or not b_L is less than zero, can be

$$\Gamma_{\rm th}^{(1)}\approx\frac{|b_L|}{a_L}\approx\frac{W_R^2+W_RW-W^2}{W+W_R} ,$$

which is independent of W_{21}, or

$$\Gamma_{\rm th}^{(1)}\approx-\frac{|c_L|}{|b_L|}\approx\frac{W^2}{W_R^2+W_RW-W^2}W_{21} ,$$

which is linearly proportional to W_{21}. Here we have also neglected W_{34} which is small for the same reason as W_{21}. By solving $b_L<0$, that is, $W_R^2+W_RW-W^2<0$, we can obtain $W_{R\rm th}^{(1)}=0.618W$. Here comes one of the important results of this paper. The atomic system with $W_R>0.618W$ can result in an efficient lasing without population inversion by the virtue of the lower-level coherence.

Physically, we contribute this high efficiency to the efficient trapping of ground-level atoms when γ_{21}/W_R is small. To illustrate this point, let us examine Eq. (2.15), the zeroth-order solutions in the high intensity limit. As γ_{21}/W_R approaches zero, the populations remain same as the ones without any coherent perturbations, while the lower-level coherence becomes $\rho_{21}^{(0)}\approx-n_g=\sqrt{n_gn_g}e^{i\pi}$. Thus the absorption due to the ground levels, $[\rho_{11}^{(0)}+\rho_{22}^{(0)}+2|\rho_{21}^{(0)}|\cos(\pi)]$, experiences a destructive interference and approaches zero. If γ_{21} were only determined by W_{21}, efficient lasing without inversion would occur no matter how small W_R is as long as the ratio of W_{21} to W_R is small. However, in the current closed system, γ_{21} is the sum of Γ and W_{21}, that is, pumping degrades the lower-level coherence. Furthermore, some population must exist in level 3 to produce laser light. That is why efficient lasing without inversion requires that W_R exceeds a certain threshold value.

Although the threshold pumping condition is independent of the Raman intensity, Raman intensity does have to reach a certain threshold before any laser action takes place. This threshold is determined by Eq. (3.5). Figure 3 displays the relationship between $I_{r\rm th}^{(1)}$ and the atomic transition frequency Ω_{21} of the lower energy levels for different W_{21} when $W_R=2W$. To understand the features in Fig. 3, we note that the scale of the high intensity is measured by Eq. (2.14), not $\gamma_R^2+\Delta_R^2$, the saturation intensity in the traditional two-level system. That explains why, first, the lowest threshold appears when the

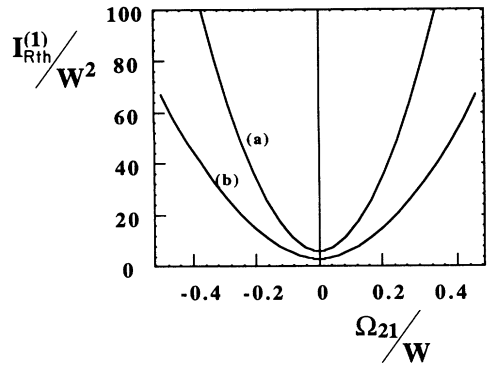

FIG. 3. Threshold Raman intensity for amplification, $I^{(1)}_{Rth}$, as a function of Ω_{21}. The parameters are $W=1$, $W_R=2$, $W_{21}=0.01$, $W_{34}=0.0001$, and (a) $\Gamma=0.005$, or equivalently $\gamma_{21}=0.015$; (b) $\Gamma=0.01$, or equivalently $\gamma_{21}=0.02$.

two lower levels are degenerate, and second, $I^{(1)}_{Rth}$ becomes more sensitive to Ω_{21} as γ_{21} decreases.

In summary, an efficient lasing without inversion consists of three conditions: $\Gamma > \Gamma^{(1)}_{th}$, $I_R > I^{(1)}_{Rth}$, and $W_R > W^{(1)}_{Rth}$.

B. Conditions for electromagnetically induced transparency

To see that the electromagnetically induced transparency is possible in this model, let us make a plot of $I^{(1)}_{Rth}$ as a function of Γ ($>\Gamma^{(1)}_{th}$) shown in Fig. 4. This figure shows that when Γ is above but very close to $\Gamma^{(1)}_{th}$, $I^{(1)}_{Rth}$ becomes extremely large. Actually, $I^{(1)}_{Rth}$ becomes infinity when $\Gamma=\Gamma^{(1)}_{th}$, which implies that no matter how large the Raman intensity, the absorption around $\Delta=\Delta_R$ can only approach zero. Thus, we conclude that the condition for the electromagnetically induced transparency is $\Gamma=\Gamma^{(1)}_{th}$. As shown in Figs. 5(a) and 5(b), when Γ is operated at $\Gamma^{(1)}_{th}$, the frequency regime between the two absorption bands, separated by a frequency range of $2d_0$ [Eq. (2.19)], becomes transparent. The transparent regime continues to be widened as Raman intensity increases.

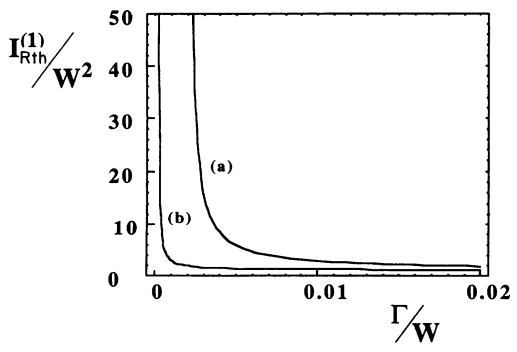

FIG. 4. Threshold Raman intensity for amplification, $I^{(1)}_{Rth}$, as a function of pumping rate Γ. The parameters are $W=1$, $W_R=2$, $W_{34}=0.0001$, and (a) $W_{21}=0.01$; (b) $W_{21}=0.001$.

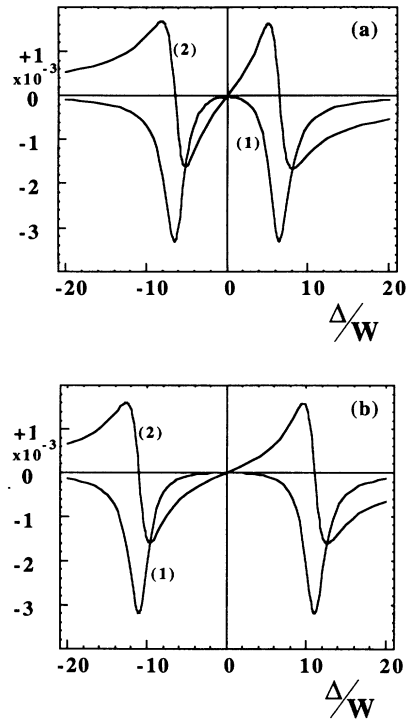

FIG. 5. Curves (1) and (2) in (a) and (b) are the absorption and dispersion spectra with $I_R=20$ and $I_R=60$, respectively. The rest parameters are $W=W_R=1$, $W_{12}=0.01$, $W_{34}=0.0001$, $\Omega_{21}=0$, and $\Gamma=\Gamma^{(1)}_{th}=0.009\,624\,68$.

C. Absorption-dispersion relations: Conditions for the largest index of refraction without absorption

The linear complex absorption coefficient is commonly governed by

$$\frac{in}{x+i\gamma}\ , \tag{3.10a}$$

or equivalently

$$n\frac{\gamma}{x^2+\gamma^2}+in\frac{x}{x^2+\gamma^2}\ , \tag{3.10b}$$

where x is the frequency detuning relative to the resonance line, n is an x-independent variable, and γ is the transverse decay rate. In the traditional two-level system, n is a real number proportional to the population difference between the two levels. That is why the absorption spectrum has the real Lorentzian line shape [first term of Eq. (3.10b)], which is an even function of frequency shift (relative to the line center), while the dispersion spectrum is governed by the imaginary Lorentzian line shape [second term of Eq. (3.10b)], which is antisymmetric. In such a medium, the largest absorption (or gain) always appears at zero dispersion. However, n can be complex in the multilevel multiphoton interaction due to the interferences among different pathways. The spectra of the absorption and dispersion in such a medium become the mixture of the real and the imaginary Lorentzian functions. More specifically, let us assume $n=n_R+in_I$; then Eq. (3.10b) becomes

$$\left[n_R \frac{\gamma}{x^2+\gamma^2} - n_I \frac{x}{x^2+\gamma^2} \right] + i \left[n_R \frac{x}{x^2+\gamma^2} + n_I \frac{\gamma}{x^2+\gamma^2} \right] . \quad (3.11)$$

The terms associated with n_R have the usual dispersion and absorption relations (Lorentzian type), while the terms associated with n_I have a dispersionlike absorption and an absorptionlike dispersion (Rayleigh-wing-type) spectra. With proper values of n_R and n_I, it is not difficult to see that the maximum dispersion can happen at frequency detuning where absorption is zero. In particular, if $n_R=0$, the spectra are purely Rayleigh wing type, and thus, the maximum dispersion always happens at zero absorption. In the case of the Raman-driven model, the spectra [Eqs. (2.18), (2.20), and (2.21)] are made up of two line shapes located around $\Delta=d_0$ and $\Delta=-d_0$. Each line shape has a similar form as Eq. (3.11) with g_R and g_L playing the role of n_R and n_I. The spectra are mainly of Lorentzian type if $|g_R| \ll |g_L|$; otherwise, they are of Rayleigh wing type. Because in the high-intensity limit both A_1 and A_2 become Raman-intensity independent, g_R, according to Eq. (2.19), is inversely proportional to the Raman field strength, while g_L (equal to A_2) is Raman-intensity independent. Therefore, as the Raman intensity increases, the spectra change from Rayleigh type to Lorentzian type.

We now proceed to derive the conditions for the largest index of refraction without absorption. We first note that the absorption is zero at

$$\Delta = \left[\frac{A_1\gamma_{34}(\gamma\gamma_{34}+2I_R)}{A_1\gamma_{34}-A_2(\gamma_{34}+\gamma)} \right]^{1/2} , \quad (3.12)$$

which is derived by setting Eq. (2.20) zero, and that the index of refraction is largest when $\partial[\mathrm{Im}(\alpha)]/\partial\Delta=0$. With these considerations, we are able to find a single implicit equation for I_R (see Appendix B for the details),

$$(\gamma_{34}\gamma+2I_R)A_2[2A_1\gamma_{34}-A_2(\gamma_{34}+\gamma)] + A_1\gamma_{34}(\gamma_{34}+\gamma)[A_1\gamma_{34}-A_2(\gamma_{34}+\gamma)]=0 . \quad (3.13)$$

Because of the lasing condition and the real value requirement of Δ in Eq. (3.12), A_1, $A_1\gamma_{34}-A_2(\gamma_{34}+\gamma)$, and $2A_1\gamma_{34}-A_2(\gamma_{34}+\gamma)$ must all be positive. As a result, Eq. (3.13) can be satisfied only under the condition that

$$A_2<0 , \quad (3.14)$$

which can be similarly handled (see Appendix C) as the lasing condition $A_1>0$. Note that we have approximated the lasing condition [Eq. (3.1)] with $A_1>0$ by dropping the term $\Delta_r\mathrm{Im}(\rho_{12}^0)$, which approaches zero at high Raman intensity. The main results in Appendix C are the three threshold values: $\Gamma_{\mathrm{th}}^{(2)}$ [Eq. (C5)], $I_{r\mathrm{th}}^{(2)}$ [Eq. (C3)], and $W_{r\mathrm{th}}^{(2)}$ [Eq. (C6)]. Similarly, $\Gamma_{\mathrm{th}}^{(2)}$ is proportional to W_{21} only if $W_R > W_{R\mathrm{th}}^{(2)}$. Curves (a) and (d) of Figs. 6 and 7 compare $\Gamma_{\mathrm{th}}^{(2)}$ with $\Gamma_{\mathrm{th}}^{(1)}$ and $\Gamma_{\mathrm{th}}^{(2)}$ with $I_{R\mathrm{th}}^{(1)}$, respectively. These figures clearly show that $\Gamma_{\mathrm{th}}^{(2)}$, $I_{R\mathrm{th}}^{(2)}$, and $W_{R\mathrm{th}}^{(2)}$ are always larger than their counterparts. This is due to the fact that A_1, compared with A_2, contains an additional gain via upper-level coherence. Simultaneous considerations of lasing condition and inequality (3.14) lead to the conclusion that the largest index of refraction at zero absorption is possible only if $\Gamma>\Gamma_{\mathrm{th}}^{(1)}$ and $I_{R\mathrm{th}}^{(1)}<I_R<I_{R\mathrm{th}}^{(2)}$, which is the parameter regime between curves (d) and (a) in Fig. 7. The exact values of I_R and Δ at which the largest index refraction occurs at zero absorption is determined by first solving Eq. (3.13) for I_R, and then plugging I_R into Eq. (3.12) for Δ.

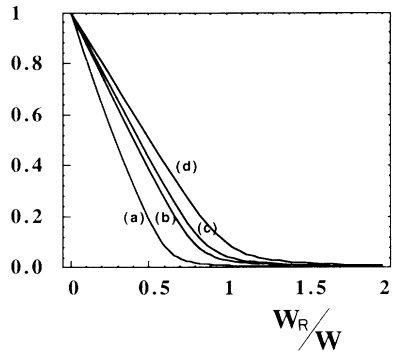

FIG. 6. Threshold Raman intensity: (a) $I_{R\mathrm{th}}^{(1)}$; (b) $I_{R\mathrm{th}}^{(D)}(f\,\delta\omega)$, where $f\,\delta\omega=10$; (c) $I_{R\mathrm{th}}^{(D)}(f\,\delta\omega)$, where $f\,\delta\omega=40$; (d) $I_{R\mathrm{th}}^{(2)}$ as a function of Γ. The parameters are $W=1$, $W12=0.01$, $W_{34}=0.0001$, and $\Omega_{21}=0$.

Finally, we point out that if $\Gamma=\Gamma_{\mathrm{th}}^{(2)}$, A_2 approaches zero for large Raman intensity. Under this condition, the spectra are always near ideal Rayleigh wing type, and the largest index refraction always occurs at near-zero absorption as long as the Raman intensity remains strong enough, as shown in Figs. 8(a) and 8(b).

D. Doppler-shift effect

In this section, we discuss the effect of Doppler broadening on the lasing condition with the help of the

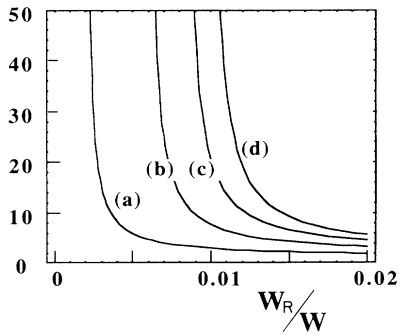

FIG. 7. Threshold pumping rate: (a) $\Gamma_{\mathrm{th}}^{(1)}$; (b) $\Gamma_{\mathrm{th}}^{(D)}(f\,\delta\omega)$, where $f\,\delta\omega=5$; (c) $\Gamma_{\mathrm{th}}^{(D)}(f\,\delta\omega)$, where $f\,\delta\omega=20$; (d) $\Gamma_{\mathrm{th}}^{(2)}$ as a function of W_R. The parameters are $W=1$, $W_{12}=0.01$, $W_{34}=0.0001$, and $\Omega_{21}=0$.

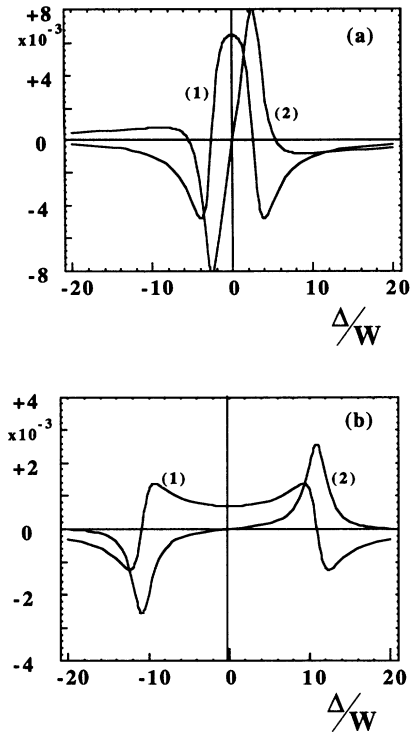

FIG. 8. Curves (1) and (2) in (a) and (b) are the absorption and dispersion spectra with I_R and $I_R=60$, respectively. The rest parameters are $W=W_R=1$, $W_{12}=0.01$, $W_{34}=0.0001$, $\Omega_{21}=0$, and $\Gamma=\Gamma_{\rm th}^{(2)}=0.095\,174\,9$.

equations in Sec. II B. Note that the formulas in Sec. II B are derived under Lorentzian instead of Gaussian functions. Therefore, the quantitative results in this section only have qualitative meanings. However, we expect that the general observations made in this section should remain valid for the calculations involving Gaussian distribution function. We now derive the lasing condition

$$A_1\gamma_{34}+f\,\delta\omega A_2>0\ , \tag{3.15}$$

by setting Eq. (2.27) to be larger than zero. We note that under two conditions Eq. (3.15) degenerates into $A_1>0$, the lasing condition in the absence of Doppler broadening. The first condition, as we expected, is $\delta\omega=0$, that is, no Doppler broadening. The second condition is that $f=0$, that is, $\omega_{R0}=\omega_0$, which suggests that the two-photon process involving Raman and probe fields ($\omega_{R0}<\omega_0$) can partially cancel the effect of the Doppler broadening on the threshold condition. The exact threshold values for the pumping rate and the Raman intensity can be easily derived by the same method that we used in discussing Eq. (3.15). Appendix D contains the details. Here, we summarize the results of Appendix D in Figs. 6 and 7. Curves (b) and (c) show the threshold pumping value $\Gamma_{\rm th}^{(D)}(f\,\delta\omega)$ [Eq. (D5)] as a function of W_R with different $f\,\delta\omega$ and the threshold Raman intensity $I_{R\rm th}^{(D)}(f\,\delta\omega)$ [Eq. (D3)] as a function of pumping rate with different $f\,\delta\omega$, respectively. They indicate that although, in general, the threshold values with Doppler effect, as we expected, are larger than those without Doppler effect curve (a), they are less than $\Gamma_{\rm th}^{(2)}$ and $I_{R\rm th}^{(2)}$ represented by curve (d). Again, an efficient lasing without inversion is possible when W_R exceeds a certain threshold. In the Doppler limit, that is, $\delta\omega$ is much greater than any atomic decay rates, the threshold values approach $\Gamma_{\rm th}^{(2)}$ and $I_{R\rm th}^{(2)}$, which are independent of Doppler width. We can understand this even without detailed calculations. Let us replace A_1 in Eq. (3.15) with Eq. (2.17a) and change Eq. (3.15) into

$$(1+f\,\delta\omega)A_2+\mathcal{R}_{34}^{(0)}/\gamma_{34}>0\ . \tag{3.16}$$

Because $\mathcal{R}_{34}^{(0)}$ is always positive, Eq. (3.16) is always satisfied no matter what the value of Doppler width is as long as $A_2>0$, which, of course, is the lasing condition in the Doppler limit. The main reason that the efficient lasing without inversion is possible even in the presence of Doppler effect is that the trapping is mainly due to 1-4-2 two-photon transition which is insensitive to the Doppler shift as a result of close atomic transition frequencies between 1-4 and 2-4.

IV. SUMMARY

In this paper, we have constructed a solution to the complex linear-absorption coefficient for the closed Raman-driven four-level symmetrical model. We have derived, from this solution, the spectra around and away from two-photon resonance [Eqs. (2.16), (2.20), and (2.21)] under reasonable assumptions. We found that the center region exhibits gain if $A_1>0$, and its peak value decreases with Raman intensity, and each side band (one is at $\Delta=d_0$ and the other is at $\Delta=-d_0$) is a mixture of Lorentzian- and Rayleigh-type spectra. The peak value of the Rayleigh type decreases with Raman field strength, while the peak value of the Lorentzian type remains independent of Raman intensity. In the high-intensity regime, the side band is predominated by the Lorentzian type, which exhibits gain if $A_2>0$. We thus found two sets of threshold values for the pumping rate and Raman intensity; one is $(\Gamma_{\rm th}^{(1)},I_{R\rm th}^{(1)})$ derived from $A_1>0$, and the other is $(\Gamma_{\rm th}^{(2)},I_{R\rm th}^{(2)})$ derived from $A_2>0$. A_2 consists of the single-photon absorption and the lower-level coherence. A_1 contains, besides all the terms in A_2, a positive term due to the upper-level coherence. For this reason, each member in the second set is larger than its counterpart in the first set. That also explains why the gain emerges first from the center, and virtually the entire absorptive profile can turn into a gain profile when $A_2>0$. In the following, we compare the pumping rate and the Raman intensity with these two sets of threshold values, and summarize the conditions for the various phenomena.

(1) Electromagnetically induced transparency appears if $\Gamma=\Gamma_{\rm th}^{(1)}$. Under this condition, A_1 approaches zero as Raman intensity increases, while A_2 is always negative no matter how large the Raman intensity is. Thus, the spectrum regime between the two side absorption bands becomes transparent, and increases with Raman intensity.

(2) When $\Gamma>\Gamma_{\rm th}^{(1)}$ and $I_{R\rm th}^{(1)}<I_R<I_{R\rm th}^{(2)}$, then $A_1>0$ and $A_2<0$. In this case, the gain is of Rayleigh wing type,

while the absorption is of Lorentzian type. With proper choice of the Raman intensity, the largest index of refraction can occur at the zero absorption.

(3) When $\Gamma=\Gamma_{\rm th}^{(2)}$, A_2 approaches zero for large Raman intensity. The spectra are mainly of Rayleigh wing type. The largest index of refraction always happens at near zero absorption as long as Raman intensity is sufficiently strong.

(4) If $\Gamma>\Gamma_{\rm th}^{(2)}$ and $I_R>I_{R\rm th}^{(2)}$, $A_2>0$. In this case, the positive value in the absorption spectrum are contributed by not only the Lorentzian but also the Rayleigh type of spectra. Thus, it is possible that the gain expands to the entire spectrum. Another feature in this case is that at the high-intensity limit the gain at the side band becomes mainly of the Lorentzian type and, therefore, its peak value is independent of Raman intensity.

A very important feature of the closed Raman-driven model is that $\Gamma_{\rm th}^{(1)}$ and $\Gamma_{\rm th}^{(2)}$ become proportional to W_{21} only if W_R is larger than $W_{R\rm th}^{(1)}$ and $W_{R\rm th}^{(2)}$, respectively. Hence, all the above phenomena can be realized efficiently. Two mechanisms are responsible for the small value of $\Gamma_{\rm th}^{(1)}$; one is atomic trapping, and the other is the two-photon gain. By comparison, atomic trapping is the only reason for the small value of $\Gamma_{\rm th}^{(2)}$. For this reason, $W_{\rm th}^{(2)}>W_{\rm th}^{(1)}$. The requirement on the W_R value stems from the fact that the pumping, although it increases the population on level 3, destroys the coherence of the ground doublet and makes atomic trapping of the ground doublet less efficient. Our calculation shows that $W_{R\rm th}^{(1)}$ is around $0.68W$, and $W_{R\rm th}^{(2)}$ is around W. However, according to the inherent frequency scaling of the spontaneous decay rate, W_R must be less than W (assuming it is purely radiative) because the atomic transition frequency between level 4 and the ground doublet is smaller than that between level 3 and the ground doublet. Therefore, one has to be careful, in adopting this model, to generate coherent light of higher frequencies because efficient lasing without inversion is unlikely to happen unless mechanisms are introduced to efficiently depopulate the auxiliary level.

We also derived, under suitable assumptions, the spectra in the presence of Doppler broadening. In particular, we discussed how the lasing condition is affected by the Doppler broadening. We found that lasing is possible if $\Gamma>\Gamma_{\rm th}^{(D)}(f\,\delta\omega)$ and $I_R>I_{R\rm th}^{(D)}(f\,\delta\omega)$, where $\Gamma_{\rm th}^{(1)}<\Gamma_{\rm th}^{(D)}(f\,\delta\omega)<\Gamma_{\rm th}^{(2)}$ and $I_{R\rm th}^{(1)}<I_{R\rm th}^{(D)}(f\,\delta\omega)<I_{R\rm th}^{(2)}$. The threshold values for the pumping rate and the Raman intensity approach $(\Gamma_{\rm th}^{(1)},I_{R\rm th}^{(1)})$ for small value of $\Delta\omega$ and f, and approach $(\Gamma_{\rm th}^{(2)},I_{R\rm th}^{(2)})$ for sufficiently large $\delta\omega$. The most important conclusion of this discussion is that efficient lasing without inversion can be achieved in the presence of Doppler broadening if $W_R>W_{R\rm th}^{(D)}(f\,\delta\omega)$, where $W_{R\rm th}^{(1)}<W_{R\rm th}^{(D)}(f\,\delta\omega)<W_{R\rm th}^{(2)}$. The physical origin of this conclusion can be traced to the atomic trapping which is insensitive to the Doppler shift as a result of close atomic transition frequencies between $1\leftrightarrow4$ and $2\leftrightarrow4$.

APPENDIX A

Because we believe most of the readers are familiar with the perturbative approach [16], we present not the derivation steps but the main formulas that are useful in the numerical implementation of the complex absorption coefficient under arbitrary parameters. In short, the complex absorption coefficient is

$$\alpha(\Delta,\Delta_R)=-i\frac{[-\gamma_{31}-i(\Omega_{21}-\Delta)]S_{g1}+(-\gamma_{32}+i\Delta)S_{g2}}{(-\gamma_{32}+i\Delta)[-\gamma_{31}-i(\Omega_{21}-\Delta)]-\dfrac{-(\gamma_{31}+\gamma_{32})+i(2\Delta-\Omega_{21})}{\gamma_{34}-i(\Delta-\Delta_R)}I_R}\,, \tag{A1}$$

where

$$S_{g1}=i(\rho_{22}^{(0)}-\rho_{33}^{(0)})+i\rho_{12}^{(0)}-E_R\frac{\rho_{24}^{(0)}+\rho_{14}^{(0)}}{\gamma_{34}-i(\Delta-\Delta_R)}\,, \tag{A2}$$

$$S_{g2}=i(\rho_{11}^{(0)}-\rho_{33}^{(0)})+i\rho_{21}^{(0)}-E_R\frac{\rho_{24}^{(0)}+\rho_{14}^{(0)}}{\gamma_{34}-i(\Delta-\Delta_R)}\,, \tag{A3}$$

The zeroth-order populations in Eqs. (A2) and (A3) are determined by equations

$$C_{34}\rho_{44}^{(0)}+C_{32}\rho_{22}^{(0)}+C_{31}\rho_{11}^{(0)}=W_{32}+W_{31}+W_{34}\,,$$

$$C_{24}\rho_{44}^{(0)}+C_{22}\rho_{22}^{(0)}+C_{21}\rho_{11}^{(0)}=W_{32}\,,$$

$$C_{14}\rho_{44}^{(0)}+C_{12}\rho_{22}^{(0)}+C_{11}\rho_{11}^{(0)}=W_{31}\,,$$

where

$$C_{34}=W_{32}+W_{31}+W_{34}\,,$$

$$C_{32}=\Gamma_{23}+W_{32}+W_{31}+W_{34}\,,$$

$$C_{31}=\Gamma_{13}+W_{32}+W_{31}+W_{34}\,,$$

$$C_{24}=-[-W_{32}+W_{42}+2I_R\mathrm{Re}(A_{24})]\,,$$

$$C_{22}=W_{21}+\Gamma_{23}+W_{32}+2I_R[\mathrm{Re}(A_{24})+I_R\mathrm{Re}(B_{24})]\,,$$

$$C_{21}=-[W_{12}-W_{32}+2I_R^2\mathrm{Re}(B_{24})]\,,$$

$$C_{14}=-[-W_{31}+W_{41}+2I_R\mathrm{Re}(A_{14})]\,,$$

$$C_{12}=-[W_{21}-W_{31}+2I_R^2\mathrm{Re}(B_{14})]\,,$$

$$C_{11}=W_{12}+\Gamma_{13}+W_{31}+2I_R[\mathrm{Re}(A_{14})+I_R^2\mathrm{Re}(B14)]\,.$$

Here,

$$A_{24}=\frac{\gamma_{21}+i(\Omega_{21}-\Delta_R)}{D},\quad A_{14}=\frac{\gamma_{21}-i\Delta_R}{D^*}\,,$$

$$B_{24}=B_{14}^*=\frac{1}{(\gamma_{21}+i\Omega_{21})D}\,,$$

and

$$D=(\gamma_{42}+i\Delta_R)[\gamma_{41}+i(\Omega_{21}-\Delta_R)]+\frac{I_R}{\gamma_{21}+i\Omega_{21}}(\gamma_{42}+\gamma_{41}-i\Omega_{21}) .$$

The zeroth-order off-diagonal elements in Eqs. (A2) and (A3) are determined as follows:

$$\rho_{24}^{(0)}=iE_R^*[A_{24}(\rho_{22}^{(0)}-\rho_{44}^{(0)})+I_R B_{24}(\rho_{22}^{(0)}-\rho_{11}^{(0)}] ,$$

$$\rho_{14}^{(0)}=iE_R^*[A_{14}(\rho_{11}^{(0)}-\rho_{44}^{(0)})+I_R B_{14}(\rho_{11}^{(0)}-\rho_{22}^{(0)})] ,$$

$$\rho_{21}^{(0)}=\frac{iE_R\rho_{24}^{(0)}-iE_R^*\rho_{41}^{(0)}}{\gamma_{21}+i\Omega_{21}} .$$

APPENDIX B

We first reorganize Eqs. (2.20) and (2.21) so that both their numerators and denominators are written as the polynomial of Δ:

$$\mathrm{Re}(\alpha)=2\frac{-\Delta^2[A_1\gamma_{34}-A_2(\gamma_{34}+\gamma)]+A_1\gamma_{34}(\gamma\gamma_{34}+2I_R)}{\Delta^4+\Delta^2(\gamma_{34}^2+\gamma^2-4I_R)+(\gamma_{34}\gamma+2I_R)^2} , \tag{B1}$$

$$\mathrm{Im}(\alpha)=2\frac{\Delta^3A_2+\Delta[A_1\gamma_{34}(\gamma_{34}+\gamma)]-A_2(\gamma\gamma_{34}+2I_R)}{\Delta^4+\Delta^2(\gamma_{34}^2+\gamma^2-4I_R)+(\gamma_{34}\gamma+2I_R)^2} . \tag{B2}$$

Zero absorption requires that Eq. (B1) be zero, that is,

$$\Delta^2=\frac{A_1\gamma_{34}(\gamma\gamma_{34}+2I_R)}{A_1\gamma_{34}-A_2(\gamma_{34}+\gamma)} . \tag{B3}$$

The condition for the largest index of refraction is derived by setting the derivative of Eq. (B2) with respect to Δ zero. With certain algebraic arrangement, we obtain

$$-A_2\Delta^6+\Delta^4[-3A_1\gamma_{34}(\gamma_{34}+\gamma)+A_2(\gamma^2+\gamma_{34}^2+3\gamma_{34}\gamma+2I_R)]+\Delta^2[-A_1\gamma_{34}(\gamma_{34}+\gamma)(\gamma^2+\gamma_{34}^2-4I_R)+A_2(\gamma_{34}\gamma+2I_R)(\gamma^2+\gamma_{34}^2+3\gamma_{34}\gamma+2I_R)]-[-A_1\gamma_{34}(\gamma_{34}+\gamma)+A_2(\gamma_{34}\gamma+2I_R)](\gamma_{34}\gamma+2I_R)^2=0 . \tag{B4}$$

By replacing Δ^2 in Eq. (B4) with Eq. (B3), we obtain

$$(2I_R+\gamma\gamma_{34})^2A_2^2[2A_1-A_2(\gamma_{34}+\gamma)]+2A_1^2A_2[A_1-A_2(\gamma_{34}+\gamma)](2I_R+\gamma\gamma_{34})+A_1^2[A_1-A_2(\gamma_{34}+\gamma)]^2(\gamma_{34}+\gamma)=0 , \tag{B5}$$

which can be factored as

$$\{(2I_R+\gamma\gamma_{34})A_2^2+A_1[A_1-A_2(\gamma_{34}+\gamma)]\}\times\{(\gamma_{34}\gamma+2I_R)A_2[2A_1\gamma_{34}-A_2(\gamma_{34}+\gamma)]+A_1\gamma_{34}(\gamma_{34}+\gamma)[A_1\gamma_{34}-A_2(\gamma_{34}+\gamma)]\}=0 . \tag{B6}$$

Because of the lasing condition and the positive value requirement on Δ^2 in Eq. (B3), A_1 and $A_1\gamma_{34}-A_2(\gamma_{34}+\gamma)$ must both be positive. Thus, the value inside the first curly bracket is always positive. Equation (B6) is satisfied only if the value inside the second curly bracket is zero.

APPENDIX C

With the help of Eqs. (2.17b) and (2.9), we can transform $A_2<0$ into

$$a_{IL}I_R^2+b_{IL}I_R+c_{IL}<0 , \tag{C1}$$

where

$$a_{IL}=-4\gamma(1+\gamma_{21}/W_R)(n_g-n_3)+4\gamma(n_g-n_4) ,$$

$$b_{IL}=-2\gamma[2(\gamma_R\gamma_{21}-\Omega_{21}\Delta_R)+\gamma_R(\gamma_{21}^2+\Omega_{21}^2)/W_R](n_g-n_3)-2[\gamma(2\Delta_R^2-\gamma_{21}\gamma_R)+\Delta_R^2(\gamma_{21}+2\gamma_R)](n_g-n_4) ,$$

$$c_{IL}=-\gamma(\Delta_R^2+\gamma_R^2)(\gamma_{21}^2+\Omega_{21}^2)(n_g-n_3) .$$

Inequality (C1) can be decomposed into two simultaneous inequalities,

$$a_{IL}=-4\gamma(1+\gamma_{21}/W_R)(n_g-n_3)+4\gamma(n_g-n_4)>0 \tag{C2}$$

and

$$I_R<I_{R\mathrm{th}}^{(2)}=(-b_{IL}+\sqrt{b_{IL}^2-4a_{IL}c_{IL}})/(2a_{IL}) . \tag{C3}$$

By using Eqs. (2.10) and (3.7), we can turn inequality (C2) into

$$a_{I\Gamma}\Gamma^2+b_{I\Gamma}\Gamma+c_{I\Gamma}>0 , \tag{C4}$$

where

$$a_{I\Gamma}=2 ,$$

$$b_{I\Gamma}=2(W_R-W)+2(W_{12}-W_{34}) ,$$

$$c_{I\Gamma}=-(2W+W_{34})W_{12} .$$

The threshold pumping rate is obtained from Eq. (C4) as

$$\Gamma_{\rm th}^{(2)}=\frac{-b_{I\Gamma}+\sqrt{b_{I\Gamma}^2-4a_{I\Gamma}c_{I\Gamma}}}{2a_{I\Gamma}} , \tag{C5}$$

which is proportional to W_{12} if $b_{I\Gamma}>0$, that is,

$$W_R > W_{Rth}^{(2)}=W . \tag{C6}$$

APPENDIX D

With the help of Eqs. (2.17b) and (2.9), we can transform $A_1+f\,\delta\omega\, A_2>0$ into

$$a_{DL}I_R^2+b_{DL}I_R+c_{DL}>0 , \tag{D1}$$

where

$$a_{DL}=-4\gamma'_{34}(1+\gamma_{21}/W_R)(n_g-n_3)$$
$$+4(\gamma'_{34}+\gamma_{21})(n_g-n_4) ,$$

$$b_{DL}=-2\gamma'_{34}[\,2(\gamma_{21}\gamma_R-\Omega_{21}\Delta_R)$$
$$+\gamma_R(\gamma_{21}^2+\Omega_{21}^2)/W_R\,](n_g-n_3)$$
$$-2[\,\gamma'_{34}(2\Delta_R^2-\gamma_{21}^2\gamma_R)$$
$$-\gamma_R(\gamma_{21}^2+\Omega_{21}^2)](n_g-n_4) ,$$

$$c_{DL}=-\gamma'_{34}(\gamma_R^2+\Delta_R^2)(\gamma_{21}^2+\Omega_{21}^2)(n_g-n_3) ,$$

and

$$\gamma'_{34}=\gamma_{34}+f\,\delta\omega .$$

Equation (D1) can be further decomposed into two simultaneous inequalities

$$a_{DL}=-4\gamma'_{34}(1+\gamma_{21}/W_R)(n_g-n_3)$$
$$+4(\gamma'_{34}+\gamma_{21})(n_g-n_4)>0 \tag{D2}$$

and

$$I_R > I_{R\rm th}^{(D)}(f\,\delta\omega)=\frac{-b_{DL}+\sqrt{b_{Dl}^2-4a_{DL}c_{DL}}}{2a_{DL}} . \tag{D3}$$

By using Eqs. (2.10) and Eq. (3.7), we can turn inequality (D2) into

$$a_{D\Gamma}\Gamma^2+b_{D\Gamma}\Gamma+c_{D\Gamma}>0 , \tag{D4}$$

where

$$a_{D\Gamma}=2(W+W_R+f\,\delta\omega) ,$$

$$b_{D\Gamma}=2W_R^2+2W_R(W+W_{12}+f\,\delta\omega)-2W^2$$
$$+W(2W_{12}-3W_{34}-2f\,\delta\omega)$$
$$-W_{34}^2+2f\,\delta\omega(W_{12}-W_{34}) ,$$

$$c_{D\Gamma}=-(2W+W_{34})(W+0.5W_{34}+f\,\delta\omega)W_{12} .$$

The threshold pumping rate is obtained from Eq. (D4) as

$$\Gamma_{\rm th}^{(D)}(f\,\delta\omega)=\frac{-b_{D\Gamma}+\sqrt{b_{D\Gamma}^2-4a_{D\Gamma}c_{D\Gamma}}}{2a_{D\Gamma}} , \tag{D5}$$

which is proportional to W_{12} if $b_{D\Gamma}>0$, that is,

$$W_R > W_{R\rm th}^{(D)}(f\,\delta\omega)$$
$$=\frac{-(W+f\,\delta\omega)+\sqrt{(W+f\,\delta\omega)(5\Omega+f\,\delta\omega)}}{2} . \tag{D6}$$

[1] V. G. Arkhipikin and Yu. I. Heller, Phys. Lett. **98A**, 12 (1983).

[2] O. Kocharovskaya and Ya. I. Khanin, Pis'ma Zh. Eksp. Teor. Fiz. **48**, 581 (1988) [JETP Lett. **48**, 630 (1988)].

[3] S. E. Harris, Phys. Rev. Lett. **62**, 1033 (1989).

[4] M. O. Scully, S.-Y. Zhu, and A. Gavrielides, Phys. Rev. Lett. **62**, 2813 (1989).

[5] L. M. Narducci, H. M. Doss, P. Ru, M. O. Scully, S. Y. Zhu, and C. Keitel, Opt. Commun. **81**, 379 (1991).

[6] L. M. Narducci, M. O. Scully, C. H. Keitel, S.-Y. Zhu, and H. M. Doss, Opt. Commun. **86**, 324 (1991).

[7] O. Kocharovskaya and P. Mandel, Phys. Rev. A **42**, 523 (1990).

[8] O. Kocharovskaya, P. Mandel, and Y. V. Radeonychev, Phys. Rev. A **45**, 1997 (1992).

[9] S. E. Harris, J. E. Field, and A. Imamoglu, Phys. Rev. Lett. **64**, 1107 (1990).

[10] S. E. Harris, J. E. Field, and A. Kasapi, Phys. Rev. A **46**, R29 (1992).

[11] M. Fleischhauer, C. H. Keitel, M. O. Scully, S. Chang, B. T. Ulrich, and Shi-Yao Zhu, Phys. Rev. A **46**, 1468 (1992).

[12] C. H. Keitel, O. A. Kocharovskaya, L. M. Narducci, M. O. Scully, and S.-Y. Zhu, Phys. Rev. A **48**, 3196 (1993).

[13] S. Y. Zhu, M. O. Scully, H. Fearn, and L. M. Narducci, Z. Phys. D **22**, 483 (1992).

[14] M. O. Scully, S. Y. Zhu, L. M. Narducci, and H. Fearn, Opt. Commun. **88**, 240 (1992).

[15] H. M. Doss, Ph.D. dissertation, Drexel University, 1992.

[16] N. Bloembergen and Y. R. Shen, Phys. Rev. **133**, A37 (1964).